The Cryosphere Discuss., 7, 4585–4632, 2013
www.the-cryosphere-discuss.net/7/4585/2013/
doi:10.5194/tcd-7-4585-2013

The Cryosphere Discussions
Open Access

Decadal trends in the Antarctic sea ice extent ultimately controlled by ice-ocean feedback

H. Goosse and V. Zunz

Université catholique de Louvain, Earth and Life Institute, Georges Lemaître Centre for Earth and Climate Research, Place Pasteur, 3, 1348 Louvain-la-Neuve, Belgium

Received: 27 August 2013 – Accepted: 4 September 2013 – Published: 11 September 2013

Correspondence to: H. Goosse (hugues.goosse@uclouvain.be)

Published by Copernicus Publications on behalf of the European Geosciences Union.

Decadal trends in the Antarctic sea ice extent

H. Goosse and V. Zunz

Abstract

The large natural variability of the Antarctic sea ice is a key characteristic of the system that might be responsible for the small positive trend in sea ice extent observed since 1979. In order to gain insight in the processes responsible for this variability, we have analysed in a control simulation performed with a coupled climate model a strong positive ice-ocean feedback that amplifies sea ice variations. When sea ice concentration increases in a region, in particular close to the ice edge, the mixed layer depth tends to decrease. This can be caused by a net inflow of ice and thus of freshwater that stabilizes the water column. Another stabilizing mechanism at interannual time scales that appears more widespread in our simulation is associated with the downward salt transport due to the seasonal cycle of ice formation: brine is released in winter when ice is formed and mixed over a deep layer while the freshwater flux caused by ice melting is included in a shallow layer, resulting in a net vertical transport of salt. Because of this stronger stratification due to the presence of sea ice, more heat is stored at depth in the ocean and the vertical oceanic heat flux is reduced, which contributes to maintain a higher ice extent. This positive feedback is not associated with a particular spatial pattern. Consequently, the spatial distribution of the trend in ice concentration is largely imposed by the wind changes that can provide the initial perturbation. A positive freshwater flux could alternatively be the initial trigger but the amplitude of the final response of the sea ice extent is finally set up by the amplification related to ice-ocean feedback. Initial conditions have also an influence as the chance to have a large increase in ice extent is higher if starting from a state characterized by a low value.

1 Introduction

In contrast to the Arctic where a strong decrease has been observed, in particular in summer, sea ice extent has slightly increased over the last decades in the Southern Ocean (Comiso and Nishio, 2008; Cavalieri and Parkinson, 2012; Parkinson and Cav-

TCD

7, 4585–4632, 2013

H. Goosse and V. Zunz

alieri, 2012). For the period November 1978–December 2010, satellite observations indicate a significant positive sea ice extent trend of $1.7 \times 10^5 \pm 2 \times 10^4$ km^2 per decade (Cavalieri and Parkinson, 2012). A positive trend is also noticed for every month, with a minimum in February at a value a bit lower than 10^5 km^2 per decade (Cavalieri and Parkinson, 2012).

The causes of this positive trend in a generally warming world are still debated. The regional distribution of the changes, characterized by a maximum increase in ice extent in the Ross Sea and a decrease in the Bellingshausen Sea (Parkinson and Cavalieri, 2012) is mainly driven by the winds but their effect on the total ice extent is less clear (e.g., Liu et al., 2004; Lefebvre et al., 2004; Goosse et al., 2009; Holland and Kwok, 2012; Simpkins et al., 2012). Modifications in the hydrological cycle of the Southern Ocean could contribute to the observed positive trend (e.g., Liu and Curry, 2010; Bintanja et al., 2013): higher snowfalls induce a higher albedo as well as snow ice formation leading to an increase in ice thickness (e.g., Fichefet and Morales Maqueda, 1999); larger precipitation rates lead to a lower sea surface salinity, a stronger oceanic stratification, a reduction in the vertical oceanic heat transport that favors ice formation (e.g., Martinson, 1990; Fichefet and Morales Maqueda, 1999; Marsland and Wolff, 2001). Enhanced melting of the Antarctic ice sheet, in particular of the ice shelves, also induces a freshwater transport towards the ocean which could lead to a decrease in surface salinity and an increase in sea ice extent in a similar way as larger precipitation (e.g. Jacobs et al., 2002; Swingedouw et al., 2008; Bintanja et al., 2013; Swart and Fyfe, 2013).

In response to natural and anthropogenic forcings, climate models simulate a weak decrease of the ice extent over the past decade (e.g., Lefebvre and Goosse, 2008a; Turner et al,. 2013; Zunz et al., 2013; Mahlstein et al., 2013). The disagreement with the observed increase might be due to the misrepresentation in models of some important feedbacks, related for instance to changes in wind patterns or in the freshwater cycle in a warmer world, as well as to the absence of a net meltwater input from the Antarctic ice sheet in the large majority of the global climate models (e.g., Liu and Curry, 2010;

Bintanja et al., 2013; Mahlstein et al., 2013; Swart and Fyfe, 2013). Alternatively, the observed positive trend of sea ice extent might be the manifestation of the large internal variability of the climate system in the Southern Ocean that would overwhelm the effect of the forcing associated with a weak decrease of the ice extent. Unfortunately, time series of observed ice extent are too short in the Southern Ocean to precisely quantify the magnitude of its multi-decadal variability. Besides, a few models display an increase in ice extent when both the response to the forcing and the internal variability of the system are taken into account. A dominant role of the internal variability in the recent changes in sea ice in the Southern Ocean is thus marginally compatible with simulated results but models have clear biases in their representation of both the mean state and the variability of the sea ice there, making the validity of this hypothesis relatively uncertain (Zunz et al., 2013; Mahlstein et al., 2013; Swart and Fyfe, 2013; Polvani and Smith, 2013).

Numerous studies have been devoted to the interannual variability of the sea ice in the Southern Ocean, describing in detail the response of the system to the dominant modes of atmospheric variability (e.g., Stössel and Kim, 1998; Timmermann et al., 2002; Liu et al., 2004; Lefebvre et al., 2004; Holland and Raphael, 2006; Zhang, 2007, Yuan and Li, 2008; Simpkins et al., 2012). The multi-centennial variability has also been investigated, focusing on the causes and on the large scale impact of changes in deep convection and deep water formation in the Southern Ocean (e.g., Mikolajewicz and Maier-Reimer, 1990; Stöessel and Kim, 2001; Santoso and England, 2006; Martin et al., 2013). Besides, although several recent studies have quantified the simulated internal variability in the framework of analyses of the changes over the last decades (e.g., Zunz et al., 2013; Mahlstein et al., 2013; Swart and Fyfe, 2013; Polvani and Smith, 2013), only a few analysis have explicitly looked at mechanisms responsible for variability at multi-decadal time scale (e.g., Beckmann and Timmermann, 2001).

Our goal here is thus to specifically analyse those mechanisms that could lead to an increase in ice-extent similar to the one observed over the last 30 yr. We will particularly focus on ice-ocean interactions because of their large role in the Southern Ocean dynamics (e.g.; Gordon, 1981; Martinson, 1990; Goosse and Fichefet, 1999; Bitz et al., 2006; Zhang, 2007; Goosse et al. 2009; Kirkman and Bitz, 2010). This will be achieved by describing first the dominant processes in a long control simulation (i.e. using constant forcing) performed with a coupled climate model. In a second step, we will determine how those processes contribute to the trend simulated over the last decades in a simulation obtained with the same model constrained to follow the observed changes using data assimilation. The model and the data assimilation technique are briefly presented in Sect. 2. Section 3 is devoted to the analysis of the multi-decadal variability of the control simulation. A simple model is used in Sect. 4 to illustrate the potential stabilization of the water column associated with sea ice formation. Section 5 is focussed on the recent changes in the simulation with data assimilation. Finally, conclusions are given in Sect. 6.

2 Methodology

2.1 Model description

The model used here is LOVECLIM (Goosse et al., 2010), a coupled climate model of intermediate complexity. Its atmospheric component is ECBilt2 (Opsteegh et al., 1998), a quasi-geostrophic model with T21 horizontal resolution (corresponding to about 5.6° by 5.6°). CLIO, the ocean component (Goosse and Fichefet, 1999), is a general circulation model with a horizontal resolution of 3° by 3°. A simple vegetation model (VECODE, Brovkin et. al., 2002) is also activated in the configuration selected here, at the same resolution as in ECBilt.

LOVECLIM has a coarser resolution than the state-of-the-art coupled general circulation models (CGCMs) and has a simplified representation of atmospheric dynamics. Nevertheless, its ocean component is a general circulation model and its sea ice model is nearly identical to LIM2, which is included in some models (e.g., Hazeleger et al., 2010; Dufresne et al., 2013) used in CMIP5 (Coupled Model Intercomparison Project, Phase 5). It simulates a seasonal cycle of the sea ice extent well in the range of the one of CGCMs (Fig. 1). Furthermore, because of its lower computational requirements, it is possible to make long spin-ups with the model until it reaches an equilibrium and thus to avoid the trouble associated with long-term drift in the Southern Ocean seen in some more sophisticated models (Sen Gupta et al., 2009, 2012; Turner et al., 2013). Finally, the model is well adapted for data assimilation using ensemble techniques and we can thus compare easily long control simulations with experiments reproducing well the recent changes thanks to the data constraint (see below).

LOVECLIM is thus an interesting tool to study the natural variability of the ice extent on multi-decadal time scales. It is well known that different models can behave quite differently in the Southern Ocean (Sen Gupta et al., 2009; Turner et al., 2013; Zunz et al., 2013; Close and Goosse, 2013). However, our goal is not to estimate quantitatively the different processes or to evaluate the skill of models in the Southern Ocean but to describe important feedbacks. It is thus easier if we base our analysis on one single model for which all the required diagnostics are available (which is generally not the case in public archives for long control runs). Nevertheless, we should ensure that our conclusions are robust and not model dependent if we want to improve our understanding of the recent changes in ice extent. To do so, the results of LOVECLIM will be briefly compared to the one of CGCMs when discussing the trend over the last 30 yr.

2.2 Data assimilation method

The data assimilation method is based on a particle filter (e.g., van Leeuwen et al., 2009) using the implementation described in Dubinkina et al. (2011) and Dubinkina and Goosse (2013). 96 members (called "particles") are propagated in time by the climate model, starting from an ensemble initialized at the year 1850. A nudging term is included to bring the surface temperature in ice free areas close to the observed one (Brohan et al., 2006), using a restoring time scale equivalent to 20 days for a depth of 50m. Every 3 months, the likelihood of each particle is then estimated as a function of the difference between the simulated temperatures and the HadCRUT3 surface air temperatures over the domain 30–90° S (Brohan et al., 2006), taking into account the information already brought by the nudging, as explained in Dubinkina and Goosse (2013). The particles are then resampled according to their likelihood, i.e. to their ability to reproduce the signal derived from the observations. The particles with low likelihood are stopped, while the particles with a high likelihood are copied a number of times proportional to their likelihood in order to keep the total number of particles constant throughout the period covered by the simulations. A small noise is added to each copy to obtain different time developments for the following period. The entire procedure is repeated sequentially until the end of the period of interest.

3 Mechanism leading to large 30-yr trends in sea ice extent in a control experiment

A 5000 yr simulation has been performed with LOVECLIM, using constant forcing corresponding to pre-industrial conditions. The last 1000 yr, which display a stable climate, are analysed in order to describe the internal processes that can lead to a multi-decadal trend in ice extent in LOVECLIM. To do so, we have identified in those 1000 simulated years 11 periods for which the ice extent is increasing at a rate of at least 10^5 km^2 per decade for each calendar months, during a minimum of 30 yr (Fig. 2). This value has been selected as it roughly corresponds to the increase observed over the period 1979–2010 analysed by Cavalieri and Parkinson (2012). Those 11 periods are scattered during the millennium analysed, with for instance four of them in the first 150 yr and none between years 300 and 500. They have also different characteristics as some display a relatively steady increase while the others have a much more variable time development.

As expected, during the periods of large positive trends in ice extent, on average, ice concentration tends to increase in all the sectors of the Southern Ocean (Fig. 3a). This is associated with a cooling of the air near the surface that reaches more than 1 °C in annual mean close to the ice edge (Fig. 3b) and a decrease in the heat content of the

TCD
7, 4585–4632, 2013

surface layer defined here as the top 200m of the water column (Fig. 3c). The strong link between those variables is confirmed by the high correlation (−0.71) between the spatial distribution of the trend of ice concentration and heat content displayed in Fig. 3a and c (Table 1). The ice also tends to become thicker on average during those periods in the majority of the regions (Fig. 3e), except in the Southern part of the Weddell Sea, but the signal is not significant there. Besides, as the thickening is larger in regions inside the pack where changes in concentration are lower, the spatial correlation between the trends in ice thickness and ice concentration is relatively low (0.36).

Despite the cooling of the air near the surface, the vertical oceanic heat flux at surface (Fig. 3f) strongly decreases in ice covered regions, with changes of more than $20\,\mathrm{W\,m^{-2}}$ in annual mean. The spatial correlation between the trend in ice concentration and in heat flux at the ocean surface reaches 0.72. Besides, off the ice edge, where the insulating barrier associated with sea ice is not present, the oceanic heat losses increase. The presence of sea ice, which limits the exchanges between the ocean and the cold atmosphere, is not the only cause of the different behaviour between ice-covered and ice free regions. The depths reached by convection is also clearly contrasted between those regions as the mixed layer becomes deeper in ice-free areas because of the surface cooling that induces higher surface densities while it becomes shallower at higher latitudes (Fig. 3g). Consequently, the entrainment of the relatively warm water at depth into the mixed layer decreases at high latitudes, the heat content of the water column at depth becomes higher (Fig. 3d), reducing the vertical oceanic heat flux and thus contributing to the maintenance of the ice at surface. The spatial correlation between the trend of heat content at depth and the one of ice concentration is lower than for surface variables, as temperature in intermediate layers is influenced by many processes, but it still reaches 0.42 on average.

The increase of the ice extent and the decrease of the depth reached by convection are associated with a surface freshening (Fig. 3h). If this salinity decrease is caused by modifications of the fluxes at the ocean surface, it could be one of the origins of the shallower mixed layer because of the decrease in surface density it induces (Fig. 4a).

TCD
7, 4585–4632, 2013

H. Goosse and V. Zunz

Alternatively, this reduced salinity could be a consequence of the changes in mixing as the entrainment at the basis of the mixed layer brings relatively salty water masses to the surface layer and any reduction of its intensity (Fig. 3g) leads to a decrease of the salinity there.

Precipitation slightly decreases in periods of large increase in ice extent (Fig. 3i), likely because of the general cooling at high latitudes. This thus acts in the opposite way compared to the observed freshening but the effect is small and not significant in the majority of the regions. Note that despite this reduction, a larger proportion of precipitation is falling in form of snow in colder conditions, leading to an increase in snow precipitation close to the ice edge (Fig. 3j). Consequently, the trend in precipitation provides a small negative feedback on the increase in sea ice extent in our experiments as it tends to destabilize the water column while snow, by bringing additional mass to the snow/sea-ice system, may contribute to a weak positive feedback.

On average, when the trend in ice extent is positive, the local net ice production integrated over one full year (thus including also melting) increases inside the pack, as the air is colder and the oceanic heat flux is lower, while it decreases close to the ice edge (Fig. 3k). This corresponds to higher melting there since the ice transport towards this region increases and ice tends to melt at lower latitudes in colder conditions. The correlation between the trend in ice concentration and the one in net ice formation is however very close to zero. This is due to the fact that, in some areas, a higher local ice formation leads, as expected at first sight, to a higher ice concentration. In some regions that are already ice covered, a higher formation is associated with higher ice thickness but no change in ice concentration. Close to the ice edge net ice formation is negative (i.e., more melting as ice is mainly present there because of the transport from southern latitudes) while ice concentration increases. Overall, the correlation between the two fields is thus very low.

Those changes in local ice formation and melting thus contribute to the decrease in salinity, the shallower mixed layer depth and the reduced vertical heat fluxes close to the ice edge (Fig. 4a). It is also responsible for the higher surface salinities in some areas at high latitudes. Nevertheless, the spatial distribution of the trends in net ice production, surface salinity and depth reached by convection display clear differences. At many locations, lower sea surface salinities and shallower mixed layer are associated with higher net ice production. This leads to a very low correlation between the spatial distribution of the trend in ice production and the depth reached by convection (0.06). More generally, the correlation between the freshwater flux at the ocean surface and the depth reached by convection is also very low (0.07). Although melting plays a role in the stabilisation of the water column in some regions, we have thus not found evidence that, at large scale, changes in surface fluxes integrated over one year are the dominant origin of the trend in ocean mixing depth inside the pack.

In many areas, the stabilization of the water column is due to other processes than the changes in annual mean surface freshwater fluxes, given that the latter tend to destabilize it. The brine release during ice formation occurs in winter when the mixed layer is deep and contributes to the mixed layer deepening. Consequently, the salt input is distributed over a relatively large depth. If the mixed layer depth was constant during the whole year and in the absence of sea ice transport, the sea ice melting in summer will perfectly compensate for this brine release and no net effect on the ocean salinity would be observed in annual mean. This is obviously not the case as the mixed layer is shallower in summer when sea ice is melting, with the ice melting being largely responsible for this shallowing. The freshwater is thus incorporated only in the top layers of the ocean (Fig. 4b). While in this example the ice melting in summer is identical to the ice formation in winter resulting in a zero mean freshwater flux, the consequence in annual mean is a net downward transport of salt, which is ultimately responsible for the deep water formation in the Southern Ocean (e.g. Gordon, 1991), in a decrease of the potential energy of the water column and in a tendency for stronger stratification and thus reduced mixed layer depths. Consequently, such a mechanism can explain how the presence of sea ice can be associated with a stronger stratification without any increase in the surface freshwater fluxes. Since its role may have been overlooked in the past, we will further investigate it using a simple model in Sect. 4.

TCD
7, 4585–4632, 2013

As a large number of studies have advocated for a dominant role of the atmospheric circulation in the changes in sea ice concentration, it might be surprising that the trend in geopotential height on average for the 11 periods is very low in our simulations and not significant in many regions (Fig. 3l). This is due to the fact that the spatial patterns of geopotential trends are very different in the 11 periods during which sea ice extent strongly increases (Fig. 5). Some are characterized by a decrease in geopotential height at high latitudes, some others by an increase. Nearly all of them present some anomalous low and high pressure systems over the Southern Ocean but the centres of action are located at different longitudes. As a result, the mean over the 11 periods is not representative of any of the period and cannot be dynamically linked with the trend in ice concentration. However, for each of the periods taken individually, many regional changes can be attributed to the atmospheric circulation. We will not go into the details here as the associated processes have already been the subject of many studies. For instance, the 4^{th} selected period is quite similar to the last decades with a decrease of geopotential over Antarctica and in the Pacific sector. This leads to southerly winds in the Ross Sea and higher ice concentration there while the northerly winds in the Bellingshausen sea cause a decrease of the ice extent in this region (Fig. 6), as discussed in several analyses devoted to the changes observed since 1979 (e.g., Liu et al., 2004; Lefebvre and Goosse, 2008b, Holland and Kwok, 2012; Simpkins et al., 2012, Parkinson and Cavalieri, 2012).

In addition to the feedbacks related to ice-ocean interactions and to the influence of the wind stress discussed above, the initial conditions at the beginning of the periods investigated also play a role in the large positive trends simulated by LOVECLIM: an increase is more likely if ice extent is initially low, the system coming back to its mean state. Indeed, the sea ice extent is on average 0.28×10^6 km^2 lower than the climatological mean of the model at the beginning of the 11 periods and 0.30×10^6 km^2 higher than this mean at the end of the periods. This means that the large positive trends generally bring the system from an anomalous low extent to an anomalous high extent, the mean over the periods being close to the long term average of the model (Fig. 2).

TCD
7, 4585–4632, 2013

Those low sea ice extent are associated with low ice concentrations, in particular in the Southern Pacific and the Weddell Sea (Fig 7a) and thus relatively warm conditions at surface (Fig. 7b). The latter may appear surprising as a high heat content at surface should prevent strong ice formation but this heat can be quickly released to the atmosphere. Besides, a lower heat content at depth (Fig. 7c) and a lower sea surface salinity (Fig. 7d) would favour an increase in ice extent as it could reduce the mixing in the water column and the vertical oceanic heat flux. The associated signal is, however, relatively weak in our simulations as those conditions could be in competition with the one that has lead to a low sea ice extent before the periods of interest. For instance, a reduced ice extent will be associated with deep mixed layer, with warm and salty water coming to the surface. Consequently, the sea surface salinity is high in some regions at the beginning of the period of ice increase (Fig. 7d) as this factor related to the low initial ice extent is dominant there compared to a reduced salinity that would also favour a large subsequent increase.

4 A simple model illustrating a possible long-term stabilization of the water column by ice formation

Sea ice is formed when the ocean is at its freezing point. This corresponds to the maximum surface density that can be reached for a given salinity in the range that is observed in the Southern Ocean. Any stabilization of the water column at the surface related to the presence of sea ice must thus ultimately be related to change in salinity. This can be first achieved by a net transport of sea ice to a particular location where it melts, induces a freshwater input at surface that reduces the salinity, increases the stratification and the stability of the water column. This horizontal transport plays thus a similar role as a positive Precipitation minus Evaporation (P – E) budget.

As discussed in Sect. 3, a stabilization can also be obtained because of purely vertical processes. This can be illustrated by means of a very simple model including two layers in the ocean and a potential ice cover (Fig. 8). It is based on the same principles

TCD
7, 4585–4632, 2013

as the one developed by Martinson et al. (1981) in their pioneer work devoted to the big Weddell polynya that occurred in 1974–1976. Similar notations will thus be used. The main difference with this previous study is that we do not focus on deep convection but rather on modest variations on the mixed layer depth. Our first layer represents the top of the ocean that is mixed every year because of the wind stirring effect or because of a destabilisation due to the increase in surface density. The second one is a layer that may be entrained in the surface mixed layer in some years, but only during the winter season and when the surface forcing is large enough. This second layer is chosen relatively thin here to mimic relatively small interannual variations of the mixed layer depth by contrast with Martinson et al. (1981) who chose a second layer several thousands of meters thick to represent specifically deep convection events. The second layer exchanges heat and salt with the deeper layers that are never included in the surface mixed layer in our simple model.

As in Martinson et al. (1981), we assume that the ice occupies the whole surface with a constant ice thickness (no leads) and neglect the seasonal variations in mixed layer depth except when it reaches the second layer. We have also made additional simplifications compared to Martinson et al. (1981), to only include the terms necessary for our purpose. We neglect the freshwater flux at surface associated with precipitation and evaporation to focus on surface fluxes due to ice formation/melting; there is no exchange by diffusion between the two layers except when the first layer becomes denser that the one below leading to an instantaneous mixing of the two layers; the heat flux at the atmosphere interface follows a simple sinusoidal law during the year and is identical if sea ice is present or not.

TCD
7, 4585–4632, 2013

The equations for the 5 model variables $T_1, T_2, S_1, S_2, \delta$, corresponding to temperature and salinity of the two layers and to ice thickness are:

$$
\begin{aligned}
h_1 \frac{\mathrm{d}T_1}{\mathrm{d}t} &= \frac{F_{\mathrm{surf}}}{\rho_0 c_\mathrm{p}} \\
h_1 \frac{\mathrm{d}S_1}{\mathrm{d}t} &= \sigma \frac{\mathrm{d}\delta}{\mathrm{d}t} \\
\frac{\mathrm{d}\delta}{dt} &= \frac{1}{\rho_\mathrm{i} L} \left(-Q_{\mathrm{surf}} - \rho_0 c_\mathrm{p} c_{\mathrm{hi}} (T_1 - T_\mathrm{F}) \right) \\
h_2 \frac{\mathrm{d}T_2}{\mathrm{d}t} &= -k_\mathrm{r} (T_2 - T_\mathrm{M}) \\
h_2 \frac{\mathrm{d}S_2}{\mathrm{d}t} &= -k_\mathrm{r} (S_2 - S_\mathrm{M})
\end{aligned}
\tag{1}
$$

using a simple linear equation of state for ocean density ρ:

$$\rho' = \frac{\rho - \rho_0}{\rho_0} = -\alpha T + \beta S. \tag{2}$$

The surface forcing Q_{surf} is given by:

$$Q_{\mathrm{surf}} = A_\mathrm{F} \cos\left(2\pi t / (365 \cdot 86400)\right). \tag{3}$$

If the ocean is ice free, the flux at the surface of the ocean F_{surf} is

$$F_{\mathrm{surf}} = Q_{\mathrm{surf}} \tag{4}$$

otherwise it is:

$$F_{\mathrm{surf}} = -\rho_0 c_\mathrm{p} c_{\mathrm{hi}} (T_1 - T_\mathrm{F}). \tag{5}$$

The meaning of the parameters as well as the values selected in the standard experiment are given in Table 2.

TCD
7, 4585–4632, 2013

As there are no net annual mean heat and freshwater fluxes at surface, an equilibrium can only be reached if there are also no net heat and salt inputs from the deep ocean in the bottom layer of the model, represented here by a restoring term with a coefficient k_r (Table 2). This can be achieved in two cases. First, the top layer is always stable, leading to no exchange between the first and second layers. The first layer evolves in response to the surface fluxes independently of the second one and of the deep ocean, while the second layer reaches after a few years the same characteristics as the deep ocean. This is for instance the case if the initial conditions display a strong stratification between the two layers that cannot be broken by the imposed surface fluxes. The second possibility, if the two layers interact, is that the mean flux due to the exchanges with the deep ocean is zero. This is achieved when the mean of T_2 and S_2 are equal to T_M and S_M, respectively.

When starting from a weakly stratified ocean at $t = 0$ ($S_1 = 34.9$, $T_1 = 0.5\,^{\circ}\mathrm{C}$, $S_2 = S_M$, $T_2 = T_M$), the system is destabilized every winter, inducing a heat input from the deep level to the surface and a warming of the first layer until the temperature T_1 becomes in winter (when there are exchanges between layer 1 and 2) close to the deep temperature T_M (Fig. 9). The water column is all year long warmer than the freezing point and no sea ice is formed. Salinity becomes homogenous and equal to the deep salinity S_M as no mechanism can restore a significant salinity difference between layer 1 and layer 2 after mixing has occurred.

If this equilibrium is perturbed by instantaneously setting $T_1 = T_F$, this leads to sea ice formation, a large increase in winter salinity because of brine release during ice formation and thus a vigorous overturning of the water column (Fig. 10). This warms the surface layer and leads to a decrease in ice formation (or to ice melting), providing a negative feedback as described in detail by Martinson (1990). The overturning also leads to a transport of salt from the top layer to the second one as mixing occurs when S_1 is high in winter while the freshwater flux due to the melting of sea ice is incorporated in the surface layer only. Consequently, the annual surface salinity decreases, up to the point where the stratification is high enough to forbid overturning. The sys-

TCD
7, 4585–4632, 2013

H. Goosse and V. Zunz

tem thus never reaches the state observed before the perturbation but a different one characterized by a shallower mixed layer depth corresponding to the first layer only, colder temperatures in the surface layer, no heat input to the surface layer from the deep ocean and a seasonal sea ice cover. In summary, the brine released by sea ice induces a negative feedback at the seasonal time scale as it destabilizes the water column and brings warmer water to the surface that reduces the initial ice formation (Martinson 1990) but on interannual timescale it has a stabilizing effect leading to a positive feedback as illustrated here.

For the same surface fluxes and deep ocean characteristics, this simple model has thus two equilibrium states: one without sea ice and one with a seasonal ice cover, and the system can shift from one to another as a result of a perturbation. We must, however, be very careful with such simple systems that can display multiple equilibrium or not, for instance in function of the type of boundary conditions that is imposed (e.g. Mikolajewicz and Maier-Reimer, 1994; Lenderink and Haarsma, 1994, 1996), or that can be strongly dependant of the parameters used. Furthermore, only one process is included here while additional feedbacks or the presence of a net surface freshwater flux can modify the existence or the stability properties of the two equilibriums. Consequently, we do not claim that some regions of the real Southern Ocean could have two equilibriums for present-day conditions, one with a seasonal ice cover and one without ice. Alternatively, we do not want to make our model more complex to be more realistic as, thanks to its simplicity, it has allowed underlining in a straightforward way the potentially powerful stabilization effect of the downward transport of salt associated with brine release in winter when mixed layer is deep and ice melting in summer when mixed layer is shallow.

5 Trend over the last decades

On average, the historical simulations performed in the framework of CMIP5 display a decrease of the ice extent over the period 1979–2005 in response to anthropogenic forcing (Turner et al., 2013; Zunz et al., 2013; Mahlstein et al., 2013). Nevertheless, a few of the individual members show a weak increase (see for instance Fig. 3 of Zunz et al., 2013). Although the respective role of the forcing and internal variability has not been assessed for the majority of models, this likely corresponds to cases where the latter is able to overwhelm the forced model response (Zunz et al., 2013; Mahlstein et al., 2013; Polvani and Smith, 2013). This is consistent with the fact that, for the models providing several members, such an increase is observed in some of the members but not in all of them.

In all those simulations, the increase in total ice extent is associated with an increase in ice concentration in some sectors of the Southern Ocean and a decrease in other regions (Fig. 11). Furthermore, the spatial distribution of the sea ice concentration trends strongly varies from one model to another and even between different simulations performed with the same model. This is in agreement with the hypothesis deduced from LOVECLIM results (see Fig.6) that a positive trend in ice extent could be obtained from very different spatial patterns.

Thanks to data assimilation, LOVECLIM can be constrained to follow the observed changes over the last decades, with a large decrease of the ice concentration in the Bellingshausen Sea and in the western Weddell Sea and an increase in the majority of the other sectors. This pattern agrees well with the observed one, although the decrease in the Bellingshausen Sea is a bit too widespread and covers a part of the Ross Sea in LOVECLIM (Fig 12a). The overall trend in ice extent is of $-38 \pm 93 \times 10^3\,\mathrm{km}^2$ per decade over the period 1979–2009. This implies that the ensemble mean of the simulation with data assimilation underestimates the observed increased but its value is much higher than the mean of an ensemble of simulations performed with LOVECLIM without data assimilation ($-152 \pm 49 \times 10^3\,\mathrm{km}^2$ per decade). The data assimilation technique applied here provides a weak constraint on model results as only surface temperature data, the HadCRUT3 dataset coming from a surface thermometric network which is very sparse at high latitudes (Brohan et al. 2006), are used. This has the advantage to introduce limited perturbations in the model dynamics (e.g., Dubinkina et al., 2011;

TCD
7, 4585–4632, 2013

Dubinkina and Goosse, 2013) and to provide estimates over the 20th century that are as homogenous as possible (Goosse et al., 2009). In comparison, the atmospheric reanalyses have often shifts in the late 1970's associated with the introduction of satellite measurements in the set of assimilated data, which leads to spurious long-term trends (Kistler et al., 2001; Fichefet et al., 2003; Marshall, 2003). Because of this weak constraint and because of the low resolution of LOVECLIM, we do not expect to reproduce the details of the observed trends. Even sea-ice-ocean models driven by the best estimates of atmospheric forcing have trouble in reproducing the sea ice variability in the Southern Ocean over the last decades (Fichefet et al., 2003; Zhang, 2007; Massonnet et al., 2012). Nevertheless, this is not critical as our main objective is not to examine the details of the spatial distribution of the changes but to focus on the processes studied in Sects. 3 and 4 in order to estimate if they have likely played a role in the recent large-scale changes of the sea-ice cover.

As discussed for the periods of large increase in sea ice extent in the control experiment, the increase in sea ice concentration in the simulation with data assimilation is larger in areas where there is a strong increase in the southerly winds, as in the western Ross Sea and eastern Weddell Sea (Fig. 12f). By contrast, the decrease is very large in the Bellingshausen Sea where the wind anomalies are southward. A decrease in the surface air temperature and in the heat content of the surface layer is also noticed in regions where ice concentration is increasing (Fig. 12b), but the signal is weaker than in the control experiment (Fig. 3c). The depth of the mixed layer is decreasing (Fig. 12d) at high latitudes except in some areas of the Bellingshausen Sea while it increases around 60° S in the Ross Sea and between 45 and 80° E. The surface salinity decreases nearly everywhere (Fig. 12e). This is associated with an increase in the oceanic heat content at depth (Fig. 12c), which is larger than in the control experiment (Fig. 3d). No clear link has been found between surface freshwater fluxes and the changes in mixed layer depth (not shown). Those results appear compatible with the combination of a general temperature increase and freshening at high latitudes associ-

TCD
7, 4585–4632, 2013

ated with the response to the forcing and the internal variability of the modelled system that tends to increase the sea ice extent as described for the control experiment.

Long time series are rare at the high latitudes of the Southern Ocean but, in the Ross Sea, a freshening at all depths over the continental shelf and a warming at intermediate depth (around 300 m) north of it have been observed since the 1970's (Jacobs et al. 2002; Orsi and Wiederwohl, 2009). At larger scale, Durack and Wijffels (2010) suggest a freshening at high latitudes in the Ross Sea sector and a salinity increase in the Bellingshausen Sea over the last 50 yr. In the Weddell Sea, the temperature of Warm Deep Water (WDW) is characterized by strong decadal fluctuations, probably linked to the variability of the oceanic circulation, but also by a small warming trend (Fahrbach et al. 2011). Although very fragmentary, those observations are generally consistent with our simulation with data assimilation (except the salinity increase in the Bellingshausen Sea) and with the mechanism proposed to explain the natural variability in LOVECLIM. This is encouraging but could not be considered as a definitive proof that the stabilization of the water column by the vertical salt transport associated with ice formation is playing a dominant role in the recent changes as many causes may trigger a positive ice-ocean feedback leading to a stronger stratification, larger heat storage at depth and lower vertical heat transfer (Fig. 4).

In the simulation with data assimilation, the sea ice extent in 1979 is very close to the mean of an ensemble of simulations without data assimilation. This suggests that the simulated changes after 1979 are not associated with the recovery from a low value, a factor that contributes to the ice extent increase in some of the periods studied in the control experiment. The simulation with data assimilation displays a decrease in ice extent between the 1960's and the late 1970's. This is consistent with earlier simulations performed with data assimilation using a simpler technique (Goosse et al., 2009), showing that this result is robust to modifications of our experimental design. The reconstructions are relatively uncertain over this period. Nevertheless, early satellite data suggest that the sea ice extent was larger in 1964 as well as in the early 1970's than after 1979 (Cavalieri et al., 2003; Meier et al., 2013). Indirect estimates based on whal-

TCD
7, 4585–4632, 2013

ing records or derived from ice core measurements are subject to larger uncertainties but they also independently suggest higher ice extent before 1979 (de la Mare, 1977; Curran et al., 2003; Cotté and Guinet, 2007; Abram et al., 2010). However, it has not been possible here to identify any link between this suggested decrease in ice extent in the 1960's and the 1970's and the observed increase since 1979.

6 Conclusions

In the simulations we have analysed, the multi-decadal variability of the Antarctic sea ice is not associated with a dominant spatial pattern. Each 30-yr period of a control simulation performed with LOVECLIM characterized by a large increase in sea ice extent displays positive trends in ice concentration in the majority of the sectors of the Southern Ocean but also negative ones in regions that differ between the periods. This conclusion is also valid for the CGCMs that show a positive trend over the last decades.

Nevertheless, two main conclusions have been derived from our experiments. First, the probability of having a period of large increase in ice extent is higher if we have initially a low sea ice extent as a return to mean conditions would already contribute to the increase, but this condition is not required in all the cases analyzed. Secondly, a higher ice extent is associated with a stabilization of the water column, storage of heat at depth, and reduced vertical oceanic heat flux. This provides a powerful feedback that amplifies the variability of the system and provides the memory required to sustain large multi-decadal variations. This stabilization can be due to a freshwater input to a region because of a net sea ice inflow or to the downward transport of salt caused by the incorporation of the brine released in winter in a deeper oceanic mixed layer than the meltwater in summer.

This important feedback has its origin in the low stratification of the Southern Ocean and in the presence of relatively warm water at depth. It has thus different magnitudes in different regions as a function of the vertical structure of the water column. However,

TCD
7, 4585–4632, 2013

it can be active in nearly all the areas at high southern latitudes, explaining why a large variability of the ice concentration can be found nearly everywhere in our experiments.

The spatial structure of any particular period of sea ice extent increase is thus conditioned by other processes. In our experiments, it is mainly governed by the winds (in agreement with what has been observed over the last decades), that brings cold air and transports sea ice, inducing the initial anomaly in sea ice concentration. Additional freshwater fluxes due to higher precipitation rates or the meltwater inflow from ice shelves are not required but they can also be the origin of additional ice formation. Nevertheless, whatever the original trigger, the amplification of the initial perturbation crucially depends on the modification in the vertical stratification caused by the presence of sea ice. We can thus state that the final magnitude of the changes are largely determined by the ice-ocean feedbacks. This dominant role of a feedback compared to the initial cause of the event also explains why it appears difficult to attribute the sea ice development observed during a particular period, as for instance the last 30 yr, to a specific origin.

It has been demonstrated that ice-ocean interactions play an essential role in the Southern Ocean at the seasonal time scale. The upward vertical heat transport associated with the mixed layer deepening due to brine rejection in winter provides a strong negative feedback that limits ice formation and a further mixed layer deepening (Martinson, 1990). The modification of sea ice freshwater and salt fluxes in response to anthropogenic forcing contributes to heat storage at depth and to a reduction of the upward heat fluxes that moderates the surface changes leading also to a negative feedback (Bitz et al., 2006; Kirkman and Bitz, 2010). By contrast, on interannual time scales, as we have illustrated here, the net downward salt transport due to ice formation provides a positive feedback that amplifies the variability of the system. This positive feedback is clearly different from the one associated with deep convection events that may lead to polynya formation or strongly reduced ice concentration (e.g., Martinson et al., 1981; Mikolajewicz and Maier-Reimer, 1990; Stöessel and Kim, 2001; Martin et al., 2013). During the years following such an event, the vertical stratification remains low

TCD
7, 4585–4632, 2013

and could easily be destroyed in winter, maintaining deep mixing during several years and potentially leading to multi-decadal variations of the sea ice extent. In the mechanism illustrated here, the modifications of the mixed layer are much weaker and no major change in the vertical structure is required. Another important difference is that such deep convection event is possible only in some restricted regions of the Southern Ocean while the downward transport of salt associated with ice formation can occur over a wide domain.

The feedback we have discussed is certainly not the only one that impacts sea ice variability (e.g. Ebert and Curry, 1993; Qu and Hall, 2006; Flanner et al., 2011; Kay et al., 2011), but it appears robust and provides a reasonable explanation for some important characteristics of the simulations performed with LOVECLIM and CGCMs as well as for the recent observations. It is based on sound physical principles and can be described in a simple model. Its exact magnitude is on the other hand relatively uncertain: it strongly depends on the mean state of the system (in particular the mean seasonal cycle of the mixed layer depth) and on the impact of surface fluxes associated with melting and freezing on vertical mixing. Current models have biases in their representation of those processes. Because of their importance, it is crucial to improve them in order to have a better understanding of the relative contribution of internal variability and of the forced response in the recent changes and thus a higher confidence in the projections for the 21st century.

Acknowledgements. We would like to thank Sally Close and Svetlana Dubinkina for their helpful comments on the manuscript. We acknowledge the World Climate Research Programme's Working Group on Coupled Modelling, which is responsible for CMIP. For CMIP the US Department of Energy's Program for Climate Model Diagnosis and Intercomparison provides coordinating support and led development of software infrastructure in partnership with the Global Organization for Earth System Science Portals. H. Goosse is Senior Research Associate with the Fonds National de la Recherche Scientifique (F.R.S. – FNRS-Belgium). V. Zunz is Research Fellow with the Fonds pour la formation à la Recherche dans l'Industrie et dans l'Agronomie (FRIA-Belgium). This work has been performed in the framework of the ESF HOLOCLIP project (a joint research project of the European Science Foundation PolarCLIMATE program, which is funded by national contributions from Italy, France, Germany, Spain, Netherlands, Belgium and the United Kingdom) and is supported by the F.R.S. – FNRS and by the Belgian Federal Science Policy Office (Research Program on Science for a Sustainable Development). Computational resources have been provided by the supercomputing facilities of the Université catholique de Louvain (CISM/UCL) and the Consortium des Equipements de Calcul Intensif en Fédération Wallonie Bruxelles (CECI) funded by the Fond de la Recherche Scientifique de Belgique (FRS-FNRS). This is HOLOCLIP contribution X1.

References

Abram, N. J., Thomas, E. R., McConnell, J. R., Mulvaney, R., Bracegirdle, T. J., Sime, L. C., and Aristarain, A. J.: Ice core evidence for a 20th century decline of sea ice in the Bellingshausen Sea, Antarctica, J. Geophys. Res., 115, D23101, doi:10.1029/2010JD014644, 2010.

Beckmann, A. and Timmermann, R.: Circumpolar influences on the Weddell Sea: Indication of an Antarctic Circumpolar Coastal Wave, J. Climate, 14, 3785–3792, doi:10.1175/1520-0442(2001)014<3785:CIOTWS>2.0.CO;2, 2001.

Bintanja, R., van Oldenborgh, G. J., Drijfhout, S. S., Wouters, B., and Katsman, C. A.: Important role for ocean warming and increased ice-shelf melt in Antarctic sea-ice expansion, Nat. Geosi., 6, 376–379, doi:10.1038/ngeo1767, 2013.

Bitz, C. M., Gent, P. R., Woodgate, R. A., Holland, M. M., and Lindsay, R.: The influence of sea ice on ocean heat uptake in response to increasing CO_2, J. Climate, 19, 2437–2450, doi:10.1175/JCLI3756.1, 2006.

Brohan P., Kennedy, J. J., Harris, I., Tett, S. F. B., and Jones, P. D.: Uncertainty estimates in regional and global observed temperature changes: A new data set from 1850, J. Geophys. Res., 111, D12106, doi:10.1029/2005JD006548, 2006.

Brovkin, V., Bendtsen, J., Claussen, M., Ganopolski, A., Kubatzki, C., Petoukhov, V., and Andreev, A.: Carbon cycle, vegetation and climate dynamics in the Holocene: experiments with the CLIMBER-2 model, Global Biogeochem. Cy., 16, 86-1–86-20, doi:10.1029/2001GB001662, 2002.

Cavalieri, D. J. and Parkinson, C. L.: Antarctic sea ice variability and trends, 1979–2006, J. Geophys. Res., 113, C07004, doi:10.1029/2007JC004564, 2008.

Cavalieri, D. J. and Parkinson, C. L.: Arctic sea ice variability and trends, 1979–2010, The Cryosphere, 6, 881–889, doi:10.5194/tc-6-881-2012, 2012.
Cavalieri, D. J., Parkinson, C. L., and Vinnikov, K. Y.: 30-year satellite record reveals contrasting Arctic and Antarctic decadal sea ice variability, Geophys. Res. Lett., 30, 1970, doi:10.1029/2003GL018931, 2003.
Close, S. and Goosse, H.: Entrainment-driven modulation of Southern Ocean mixed layer and sea ice variability in CMIP5 models, J. Geophys. Res., 118, 2811–2827, doi:10.1002/jgrc.20226, 2013.
Comiso, J. C. and Nishio, F.: Trends in the sea ice cover using enhanced and compatible AMSR-E, SSM/I, and SMMR data, J. Geophys. Res., 113, C02S07, doi:10.1029/2007JC004257, 2008.
Cotté, C. and Guinet C.: Historical whaling records reveal major regional retreat of Antarctic sea ice, Deep-Sea Res. Pt. I, 54, 243–252, doi:10.1016/j.dsr.2006.11.001, 2007.
Curran, M. A., van Ommen, T. D., Morgan, V. I., Phillips, K. L., and Palmer, A. S.: Ice core evidence for Antarctic sea ice decline since the 1950s, Science, 232, 1203–1206, doi:10.1126/science.1087888, 2003.
de la Mare, W. K.: Abrupt mid-twentieth-century decline in Antarctic sea-ice extent from whaling records, Nature, 389, 57–60, doi:10.1038/37956, 1997.
Dufresne, J. L., Foujols, M.-A., Denvil, S., Caubel, A., Marti, O., Aumont, O., Balkanski, Y., Bekki, S., Bellenger, H., Benshila, R., Bony, S., Bopp, L., Braconnot, P., Brockmann, P., Cadule, P., Cheruy, F., Codron, F., Cozic, A., Cugnet, D., de Noblet, N., Duvel, J.-P., Ethé, C., Fairhead, L., Fichefet, T., Flavoni, S., Friedlingstein, P., Grandpeix, J.-Y., Guez, L., Guilyardi, E., Hauglustaine, D., Hourdin, F., Idelkadi, A., Ghattas, J., Joussaume, S., Kageyama, M., Krinner, G., Labetoulle, S., Lahellec, A., Lefebvre, M.-P., Lefevre, F., Levy, C., Li, Z. X., Lloyd, J., Lott, F., Madec, G., Mancip, M., Marchand, M., Masson, S., Meurdesoif, Y., Mignot, J., Musat, I., Parouty, S., Polcher, J., Rio, C., Schulz, M., Swingedouw, D., Szopa, S., Talandier, C., Terray, P., Viovy, N., and Vuichard, N.: Climate change projections using the IPSL-CM5 Earth System Model: from CMIP3 to CMIP5, Clim. Dynam., 40, 2123–2165, doi:10.1007/s00382-012-1636-1, 2013
Dubinkina, S. and Goosse, H.: An assessment of particle filtering methods and nudging for climate state reconstructions, Clim. Past, 9, 1141–1152, doi:10.5194/cp-9-1141-2013, 2013.

Dubinkina, S., Goosse, H., Sallaz-Damaz, Y., Crespin, E., and Crucifix, M.: Testing a particle filter to reconstruct climate changes over the past centuries, Int. J. Bifurcat. Chaos, 21, 3611–3618, doi:10.1142/S0218127411030763, 2011.

Durack, P. and Wijffels, S. E.: Fifty-year trends in global ocean salinities and their relationship to broad-scale warming, J. Climate, 23, 4342–4362, doi:10.1175/2010JCLI3377.1, 2010.

Ebert, E. E. and Curry, J. A.: An intermediate one-dimensional thermodynamic sea ice model for investigating ice-atmosphere interactions, J. Geophys. Res., 98, 10085–10109, doi:10.1029/93JC00656, 1993.

Fahrbach, E., Hoppema, M., Rohardt, G., Boebel, O., Klatt, O., and Wisotzki, A.: Warming of deep and abyssal water masses along the Greenwich meridian on decadal timescales: The Weddell gyre as a heat buffer, Deep-Sea Res. Pt. II, 58, 2509–2523, doi:10.1016/j.dsr2.2011.06.007, 2011.

Fichefet, T. and Morales Maqueda, M. A.: Modelling the influence of snow accumulation and snow-ice formation on the seasonal cycle of the Antarctic sea-ice cover, Clim. Dynam., 15, 251–268, doi:10.1029/1999GL002397, 1999.

Fichefet, T., Tartinville, B., and Goosse, H.: Antarctic sea ice variability during 1958-1999: A simulation with a global ice-ocean model, J. Geophys. Res., 108, 3102, doi:10.1029/2001JC001148, 2003.

Flanner, M. G., Shell, K. M., Barlage, M., Perovich, D. K., and Tschudi, M. A.: Radiative forcing and albedo feedback from the Northern Hemisphere cryosphere between 1979 and 2008, Nat. Geosci., 4, 151–155, doi:10.1038/ngeo1062, 2011.

Goosse, H. and Fichefet T.: Importance of ice-ocean interactions for the global ocean circulation: a model study, J. Geophys. Res., 104, 23337–23355, doi:10.1029/1999JC900215, 1999.

Goosse, H., Lefebvre, W., de Montety, A., Crespin, E., and Orsi, A.: Consistent past half-century trends in the atmosphere, the sea ice and the ocean at high southern latitudes, Clim. Dynam., 33, 999–1016, doi:10.1007/s00382-008-0500-9, 2009.

Goosse, H., Brovkin, V., Fichefet, T., Haarsma, R., Huybrechts, P., Jongma, J., Mouchet, A., Selten, F., Barriat, P.-Y., Campin, J.-M., Deleersnijder, E., Driesschaert, E., Goelzer, H., Janssens, I., Loutre, M.-F., Morales Maqueda, M. A., Opsteegh, T., Mathieu, P.-P., Munhoven, G., Pettersson, E. J., Renssen, H., Roche, D. M., Schaeffer, M., Tartinville, B., Timmermann, A., and Weber, S. L.: Description of the Earth system model of intermediate complex-

ity LOVECLIM version 1.2, Geosci. Model Dev., 3, 603–633, doi:10.5194/gmd-3-603-2010, 2010.
Gordon, A. L.: Seasonality of Southern Ocean sea ice, J. Geophys. Res., 86, 4193–4197, 1981.
Gordon A. L.: Two stable modes of Southern Ocean winter stratification, in: Deep convection and deep water formation in the oceans, edited by: Chu, P. C. and Gascard, J. C., Elsevier Oceanography series 57, Elsevier, Amsterdam, the Netherlands, 17–35, 1991.
Hazeleger, W., Severijns, C., Semmler, T., Ştefănescu, S., Yang, S., Wang, X., Wyser, K., Dutra, E., Baldasano, J. M., Bintanja, R., Bougeault, P., Caballero, R., Ekman, A.M. L., Christensen, J. H., van den Hurk, B., Jimenez, P., Jones, C., Kållberg, P., Koenigk, T., McGrath, R., Miranda, P., Van Noije, T., Palmer, T., Parodi, J. A., Schmith, T., Selten, F., Storelvmo, T., Sterl, A., Tapamo, H., Vancoppenolle, M., Viterbo, P., and Willén, U.: EC-Earth: A seamless Earth-system prediction approach in action, B. Am. Meteorol. Soc., 91, 1357–1363, doi:10.1175/2010BAMS2877.1, 2010.
Holland, M. and Raphael, M.: Twentieth century simulation of the southern hemisphere climate in coupled models, Part II: sea ice conditions and variability, Clim. Dynam., 26, 229–245, doi:10.1007/s00382-005-0087-3, 2006.
Holland, P. R. and Kwok, R.: Wind-driven trends in Antarctic sea-ice drift. Nat. Geosci., 5, 872–875, doi:10.1038/NGEO1627, 2012.
Jacobs, S. S., Giulivi, C. F., and Mele, P. A.: Freshening of the Ross Sea during the late 20th century, Science, 297, 386–389, doi:10.1126/science.1069574, 2002.
Kay, J. E., Raeder, J. E. Gettelman, A., and Anderson, J.: The boundary layer response to recent Arctic sea ice loss and implications for high-latitude climate feedbacks, J. Climate, 24, 428–447, doi:10.1175/2010JCLI3651.1, 2011.
Kirkman IV, C. H. and Bitz, C. M.: The Effect of the Sea Ice Freshwater Flux on Southern Ocean Temperatures in CCSM3: Deep-Ocean Warming and Delayed Surface Warming, J. Climate, 24, 2224–2237, doi:10.1175/2010JCLI3625.1, 2010.
Kistler, R., Collins, W., Saha, S., White, G., Woollen, J., Kalnay, E., Chelliah, M., Ebisuzaki, W., Kanamitsu, M., Kousky, V., van den Dool, H., Jenne, R., and Fiorino, M.: The NCEP–NCAR 50–Year Reanalysis: Monthly Means CD-ROM and Documentation, B. Am. Meteorol. Soc., 82, 247–267, doi:10.1175/1520-0477(2001)082<0247:TNNYRM>2.3.CO;2, 2001.
Lefebvre, W. and Goosse, H.: Analysis of the projected regional sea-ice changes in the Southern Ocean during the 21st century, Clim. Dynam., 30, 59–76, doi:10.1007/s00382-007-0273-6, 2008a.

Lefebvre, W. and Goosse, H.: An analysis of the atmospheric processes driving the large-scale winter sea-ice variability in the Southern Ocean, J. Geophys. Res., 113, C02004, doi:10.1029/2006JC004032, 2008b.

Lefebvre, W., Goosse, H., Timmermann, R., and Fichefet, T.: Influence of the Southern Annular Mode on the sea-ice-ocean system, J. Geophys. Res., 109, C090005, doi:10.1029/2004JC002403, 2004.

Lenderink, G. and Haarsma, R. J.: Variability and Multiple Equilibria of the Thermohaline Circulation Associated with Deep-Water Formation, J. Phys. Oceanogr., 24, 1480–1493, doi:10.1175/1520-0485(1994)024<1480:VAMEOT>2.0.CO;2, 1994.

Lenderink, G. and Haarsma, R. J.: Modeling convective transitions in the presence of sea ice, J. Phys. Oceanogr., 26, 1448–1467, doi:10.1175/1520-0485(1996)026<1448:MCTITP>2.0.CO;2, 1996.

Liu, J. and Curry, J. A.: Accelerated warming of the Southern Ocean and its impacts on the hydrological cycle and sea ice. Search Results, P. Natl. Acad. Sci. USA, 107, 14987–14992, doi:10.1073/pnas.1003336107, 2010.

Liu, J., Curry, J. A., and Martinson, D. G.: Interpretation of recent Antarctic sea ice variability, Geophys. Res. Lett., 31, L02205, doi:10.1029/2003GL018732, 2004.

Mahlstein, I., Gent, P. R., and Solomon, S.: Historical Antarctic mean sea ice area, sea ice trends, and winds in CMIP5 simulations, J. Geophys. Res., 118, 5105–5110, doi:10.1002/jgrd.50443, 2013.

Marshall, G. J.: Trends in the Southern Annular Mode from observations and reanalyses, J. Climate, 16, 4134–4143, doi:10.1175/1520-0442(2003)016<4134:TITSAM>2.0.CO;2, 2003.

Marsland, S. J. and Wolff, J. O.: On the sensitivity of Southern Ocean sea ice to the surface freshwater flux: A model study, J. Geophys. Res., 106, 2723–2741, doi:10.1029/2000JC900086, 2001.

Martin, T., Park, W., and Latif, M.: Multi-centennial variability controlled by Southern Ocean convection in the Kiel Climate Model, Clim. Dynam., 40, 2005–2022, doi:10.1007/s00382-012-1586-7, 2013.

Martinson, D. G.: Evolution of the Southern Ocean winter mixed layer and sea ice: open ocean deepwater formation and ventilation, J. Geophys. Res., 95, 11641–11654, doi:10.1029/JC095iC07p11641, 1990.

Martinson, D. G., Killworth, P. D., and Gordon, A. L.: A convective model for the Weddell Polynya, J. Phys. Oceanogr., 11, 466–488, 1981.

Massonnet, F., Fichefet, T., Goosse, H., Vancoppenolle, M., Mathiot, P., and König Beatty, C.: On the influence of model physics on simulations of Arctic and Antarctic sea ice, The Cryosphere, 5, 687–699, doi:10.5194/tc-5-687-2011, 2011.

Meier, W. N., Gallaher, D., and Campbell, G. G.: New estimates of Arctic and Antarctic sea ice extent during September 1964 from recovered Nimbus I satellite imagery, The Cryosphere, 7, 699–705, doi:10.5194/tc-7-699-2013, 2013.

Mikolajewicz, U. and Maier-Reimer, E.: Internal secular variability in an ocean general circulation model, Clim. Dynam., 4, 145–156, 1990.

Mikolajewicz, U. and Maier-Reimer, E.: Mixed boundary conditions in ocean general circulation models and their influence on the stability of the model's conveyor belt, J. Geophys. Res., 99, 22633–22644, doi:10.1029/94JC01989, 1994.

Opsteegh, J. D., Haarsma, R. J., Selten, F. M., and Kattenberg, A.: ECBilt: A dynamic alternative to mixed boundary conditions in ocean models, Tellus A, 50, 348–367, doi:10.1034/j.1600-0870.1998.t01-1-00007.x, 1998.

Orsi, A. H. and Wiederwohl, C. L.: A recount of Ross Sea waters, Deep-Sea Res. Pt. II, 56, 778–795, doi:10.1016/j.dsr2.2008.10.033, 2009.

Parkinson, C. L. and Cavalieri, D. J.: Antarctic sea ice variability and trends, 1979–2010, The Cryosphere, 6, 871–880, doi:10.5194/tc-6-871-2012, 2012.

Polvani, L. M. and Smith, K. L.: Can natural variability explain observed Antarctic sea ice trends? New modeling evidence from CMIP5, Geophys. Res. Lett., 40, 3195–3199, doi:10.1002/grl.50578, 2013.

Qu, X. and Hall, A.: Assessing snow albedo feedback in simulated climate change, J. Climate, 19, 2617–2630, doi:10.1175/JCLI4186.1, 2006.

Santoso, A., England, M. H., and Hirst, A. C.: Circumpolar deep water circulation and variability in a Coupled Climate Model, J. Phys. Oceanogr., 36, 1523–1552. doi:10.1175/JPO2930.1, 2006.

Sen Gupta, A., Santoso, A., Taschetto, A. S., Ummenhofer, C. C., Trevena, J., and England, M. H.: Projected changes to the Southern Hemisphere ocean and sea ice in the IPCC AR4 climate models, J. Climate, 22, 3047–3078, doi:10.1175/2008JCLI2827.1, 2009.

Sen Gupta, A., Muir, L. C., Brown, J. N., Phipps, S. J., Durack, P. J., Monselesan, D., and Wijffels, S. E.: Climate drift in the CMIP3 Models, J. Climate, 25, 4621–4640, doi:10.1175/JCLI-D-11-00312.1, 2012.

TCD

7, 4585–4632, 2013

Decadal trends in the Antarctic sea ice extent

H. Goosse and V. Zunz

Simpkins, G. R., Ciasto, L. M., Thompson, D. W. J., and England, M. H.: Seasonal Relationships between Large-Scale Climate Variability and Antarctic Sea Ice Concentration, J. Climate, 25, 5451–5469, doi:10.1175/JCLI-D-11-00367.1, 2012.

Stössel, A. and Kim, S.-J.: An interannual Antarctic sea-ice – ocean mode, Geophys. Res. Lett., 25, 1007–1010, 1998.

Stössel, A. and Kim, S.-J.: Decadal deep-water variability in the subtropical Atlantic and convection in the Weddell Sea, J. Geophys. Res.-Oceans, 106, 22425–22440, doi:10.1029/2000JC000335, 2001.

Swart, N. C. and Fyfe, J. C.: The influence of recent Antarctic ice-sheet retreat on simulated sea-ice area trends. Geophys. Res. Lett., available online, doi:10.1002/grl.50820, 2013.

Swingedouw, D., Fichefet, T., Huybrechts, P., Goosse, H., Driesschaert, E., and Loutre, M. F.: Antarctic ice-sheet melting provides negative feedbacks on future climate warming, Geophys. Res. Lett., 35, L17705, doi:10.1029/2008GL034410, 2008.

Timmermann R., Hellmer, H. H., and Beckmann, A.: Simulations of ice-ocean dynamics in the Weddell Sea 2. Interannual variability 1985–1993, J. Geophys. Res., 107, 11-1–11-9, doi:10.1029/2000JC000742, 2002.

Turner, J., Bracegirdle, T. J., Phillips, T., Marshall, G. J., and Hosking, J. S.: An Initial Assessment of Antarctic Sea Ice Extent in the CMIP5 Models, J. Climate, 26, 1473–1484, doi:10.1175/JCLI-D-12-00068.1, 2013.

van Leeuwen, P. J.: Particle filtering in geophysical systems, Mon. Weather Rev., 137, 4089–4114, 2009.

Yuan, X. and Li, C.: Climate modes in southern high latitudes and their impact on Antarctic sea ice, J. Geophys. Res., 113, C06S91, doi:10.1029/2006JC004067, 2008.

Zhang, J.: Increasing Antarctic sea ice under warming atmospheric and oceanic conditions, J. Climate, 20, 2515–2529, doi:10.1175/JCLI4136.1, 2007.

Zunz, V., Goosse, H., and Massonnet, F.: How does internal variability influence the ability of CMIP5 models to reproduce the recent trend in Southern Ocean sea ice extent?, The Cryosphere, 7, 451–468, doi:10.5194/tc-7-451-2013, 2013.

TCD

7, 4585–4632, 2013

Decadal trends in the Antarctic sea ice extent

H. Goosse and V. Zunz

Table 1. Correlation between ice concentration trend and other model variables.

	Correlation for the mean over the 11 periods	Mean correlation for all the 11 periods
Oceanic heat content in the top 200 m	−0.71	−0.63
Oceanic heat content between 200 and 500 m	0.42	0.10
Ice thickness	0.36	0.35
Heat flux at the ocean surface	0.72	0.49
Depth reached by convection	−0.52	−0.30
Sea surface salinity	−0.66	−0.44
Net ice production	0.002	−0.08
Net freshwater flux at the ocean surface	0.10	0.12
Snow precipitation	0.37	0.11

Correlation between the 30-year trends in ice concentration at each grid point that is ice covered and the trend in several variables at the same location during the periods of large increase in ice extent. The first column represents the correlation applied on the average over the 11 periods while for the second column all the periods are considered individually in the analysis.

TCD
7, 4585–4632, 2013

Table 2. Description of the parameters used in the simple model.

Symbol	Parameter	Value
σ	Difference between ocean and sea ice salinity	30
ρ_i	Density of sea ice	$900\,\mathrm{kg\,m^{-3}}$
L	Latent heat of fusion of ice	$2.5\times10^5\,\mathrm{J\,kg^{-1}}$
ρ_0	Standard density of the ocean	$10^3\,\mathrm{kg\,m^{-3}}$
c_p	Heat capacity of sea water	$4\times10^3\,\mathrm{J\,K^{-1}\,kg^{-1}}$
c_{hi}	Heat exchange coefficient between ocean and sea ice	$3\times10^{-4}\,\mathrm{m\,s^{-1}}$
k_r	Strength of the nudging	h_2/(6 months)
α	Thermal expansion coefficient	$5.8\times10^{-5}\,\mathrm{K^{-1}}$
β	Haline contraction coefficient	8×10^{-4}
T_F	Freezing point temperature	$-1.8\,^{\circ}\mathrm{C}$
h_1	Thickness of the first model level	50 m
h_2	Thickness of the second model level	10 m
T_M	Deep ocean temperature	$-0.5\,^{\circ}\mathrm{C}$
S_M	Deep ocean salinity	35
A_F	Amplitude of the seasonal cycle of the surface heat flux	$100\,\mathrm{W\,m^{-2}}$

TCD
7, 4585–4632, 2013

Table 3. Model name and modelling centre corresponding to the CGCMs used to study the trend in sea ice extent over the period 1979–2005.

Model name	Institute ID	Modelling center
BCC-CSM1.1	BCC	Beijing Climate Center, China Meteorological Administration
CSIRO-Mk3.6.0	CSIRO-QCCCE	Commonwealth Scientific and Industrial Research Organization in collaboration with Queensland Climate Change Centre of Excellence
GFDL-CM3	NOAA GFDL	NOAA Geophysical Fluid Dynamics Laboratory
IPSL-CM5A-LR	IPSL	Institut Pierre-Simon Laplace
IPSL-CM5A-MR	IPSL	Institut Pierre-Simon Laplace
MRI-CGCM3	MRI	Meteorological Research Institute

TCD
7, 4585–4632, 2013

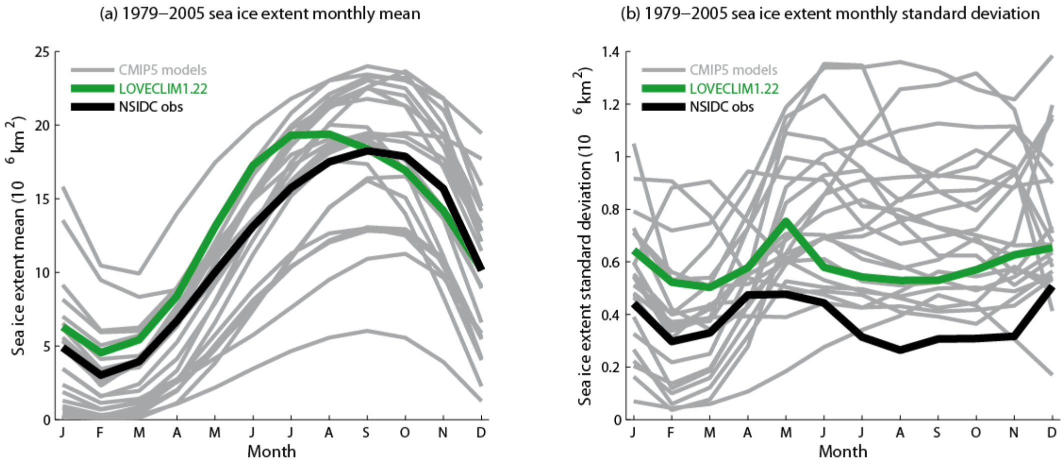

Fig. 1. (a) Monthly mean Antarctic sea ice extents as computed from LOVECLIM (in green) and 24 CGCMs (in grey) participating in CMIP5 (Coupled Model Intercomparison Project Phase 5) over the period 1979–2005. **(b)** Standard deviations of the detrended Antarctic sea ice extents as computed from LOVECLIM and the CMIP5 models over the period 1979–2005 for each month of the year. Black bold line refers to observations of Cavalieri and Parkinson (2008). This figure is adapted from Zunz et al. (2013) where the list of the models analysed can be found.

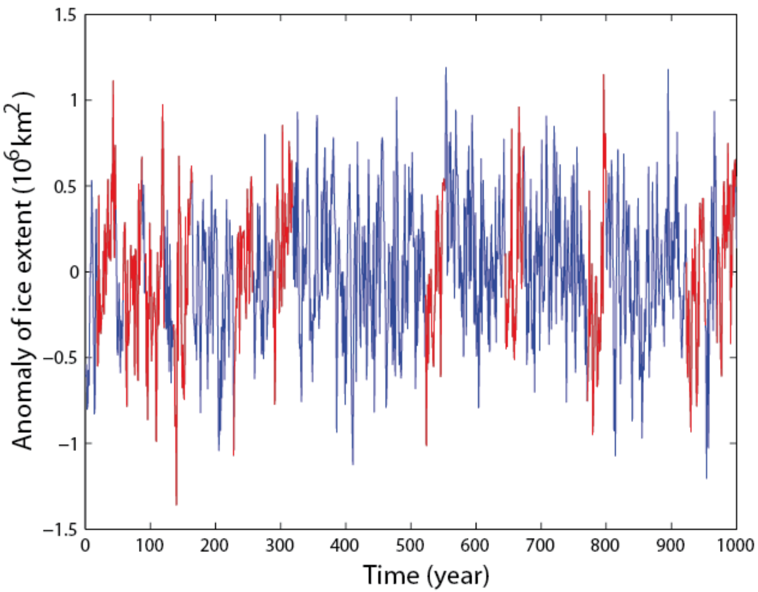

Fig. 2. Time series of the anomaly of annual mean sea ice extent in a long control run performed with LOVECLIM with regard to the mean over the full period investigated. The 11 periods characterised by an increase at a rate larger than 10^5 km^2 per decade during 30 yr in each month of the year are in red.

TCD
7, 4585–4632, 2013

H. Goosse and V. Zunz

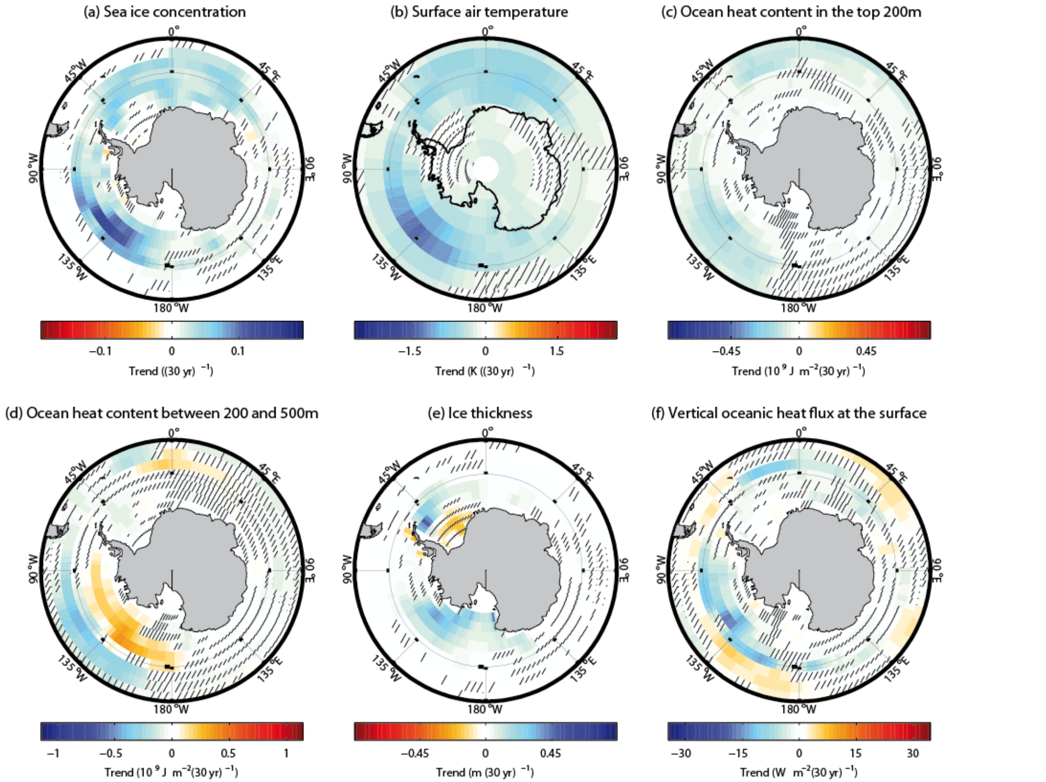

Fig. 3. Trends of annual means averaged over the 11 periods showing a large increase in Antarctic sea ice extent scaled to represent the 30 yr changes of **(a)** ice concentration, **(b)** surface air temperature (K) **(c)** ocean heat content in the top 200 m ($J\,m^{-2}$), **(d)** ocean heat content in the layer between 200 and 500 m ($J\,m^{-2}$), **(e)** ice thickness (m), **(f)** vertical oceanic heat flux at the ocean surface (positive upward, $W\,m^{-2}$).

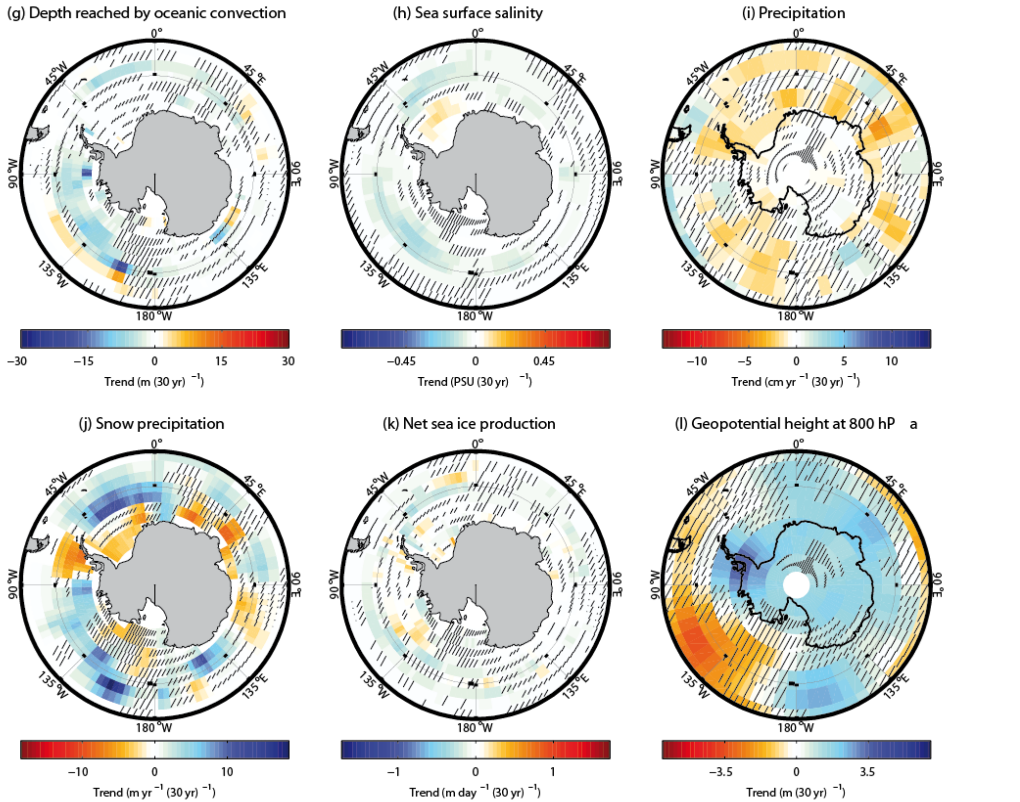

Fig. 3. (g) Depth reached by oceanic convection (m), **(h)** sea surface salinity, **(i)**, precipitation (cm yr^{-1}) **(j)**, snow precipitation (cm yr^{-1}), **(k)** net sea ice production (production minus melting) (m yr^{-1}), **(l)** geopotential height at 800 hpa (m). The hatched areas represent the regions for which the average trend over the 11 periods is not significantly different at the 95 % level from the mean trend in periods of identical length but not showing a large increase in ice extent.

TCD
7, 4585–4632, 2013

Decadal trends in the Antarctic sea ice extent

H. Goosse and V. Zunz

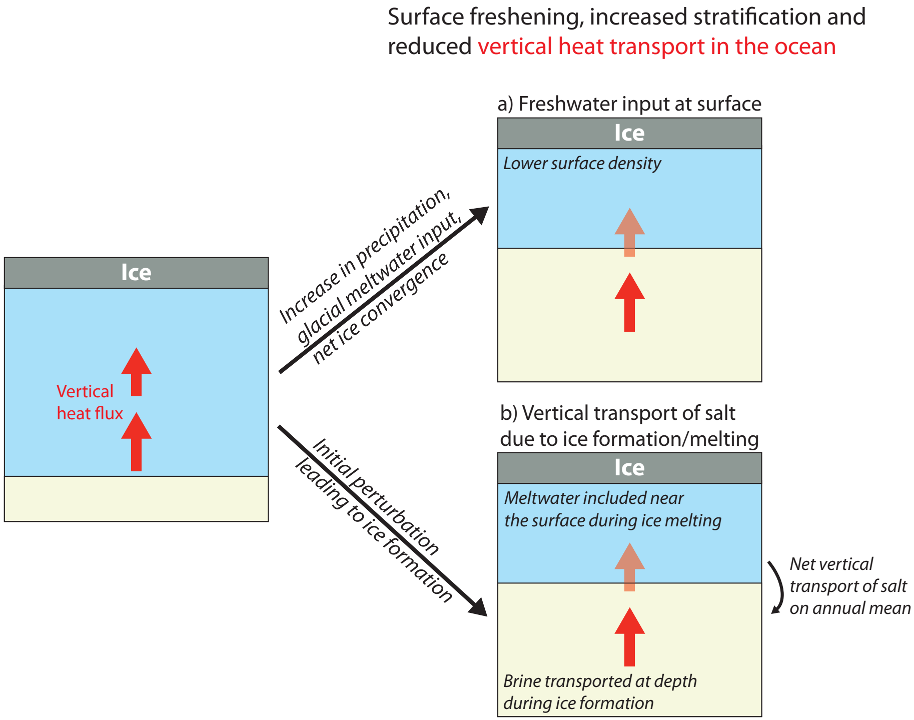

Fig. 4. Schematic representation of the stabilization of the Southern Ocean by sea ice processes

TCD
7, 4585–4632, 2013

Decadal trends in the Antarctic sea ice extent

H. Goosse and V. Zunz

Title Page
Abstract | Introduction
Conclusions | References
Tables | Figures
◂ | ▸
Back | Close
Full Screen / Esc
Printer-friendly Version
Interactive Discussion

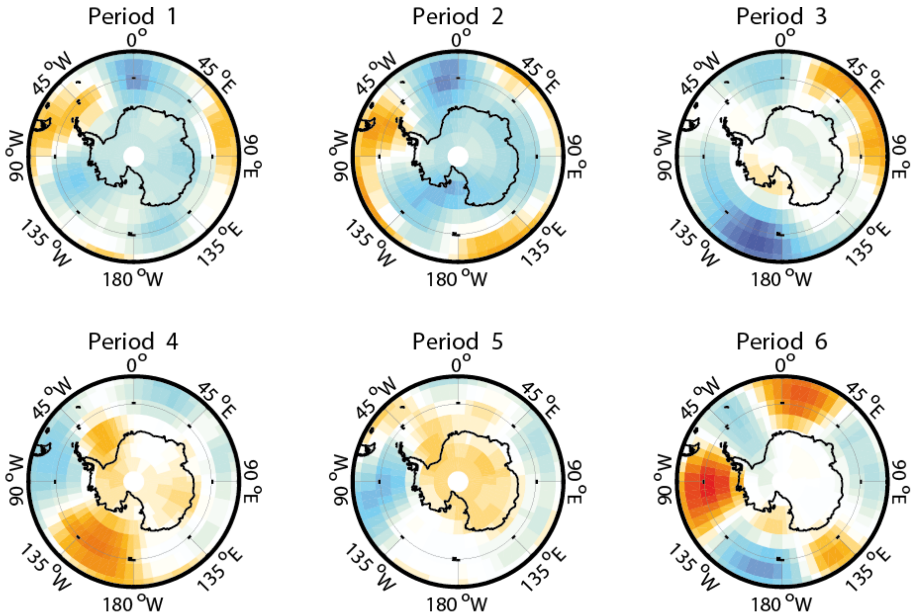

Fig. 5. Trends in geopotential height at 800 hpa (m) for the 11 periods showing a large increase in Antarctic sea ice extent scaled to represent the 30 yr changes.

TCD
7, 4585–4632, 2013

H. Goosse and V. Zunz

Title Page
Abstract | Introduction
Conclusions | References
Tables | Figures
◂ | ▸
Back | Close
Full Screen / Esc
Printer-friendly Version
Interactive Discussion

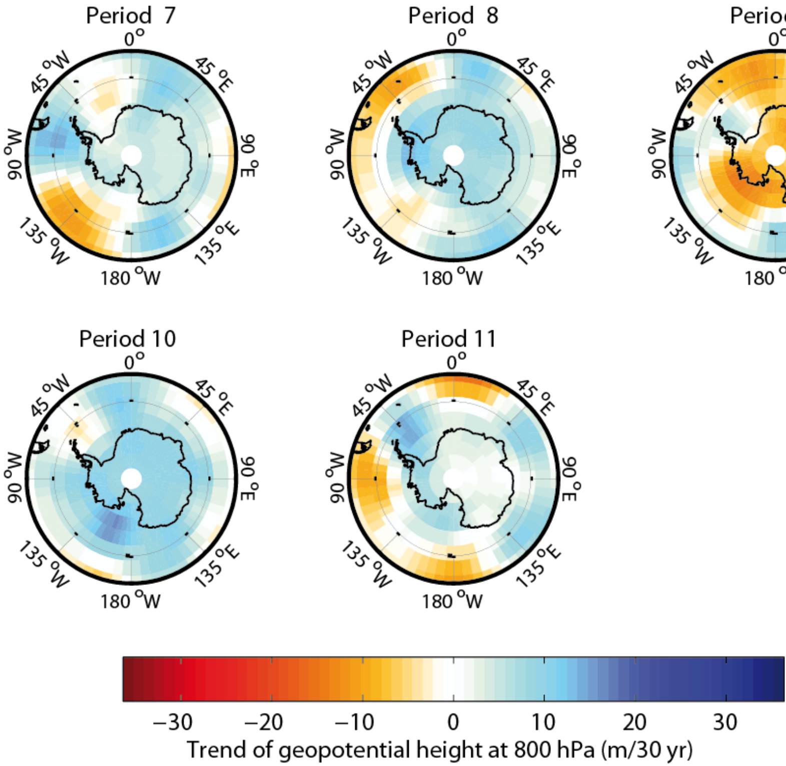

Fig. 5. Continued.

TCD
7, 4585–4632, 2013

Decadal trends in the Antarctic sea ice extent

H. Goosse and V. Zunz

Title Page
Abstract | Introduction
Conclusions | References
Tables | Figures
◀| |▶
◀ ▶
Back | Close
Full Screen / Esc
Printer-friendly Version
Interactive Discussion

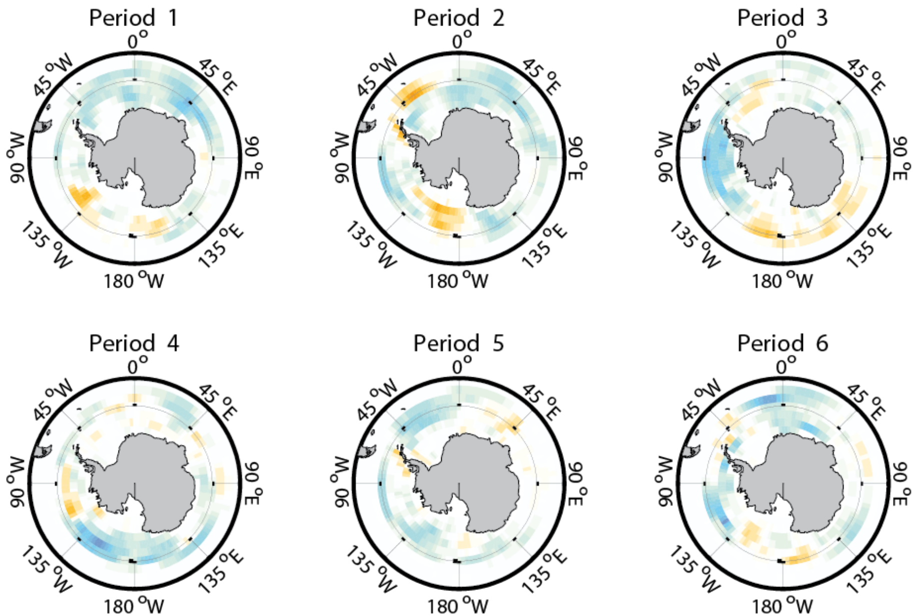

Fig. 6. Trends of annual means ice concentration for the 11 periods showing a large increase in Antarctic sea ice extent scaled to represent the 30 yr changes.

TCD
7, 4585–4632, 2013

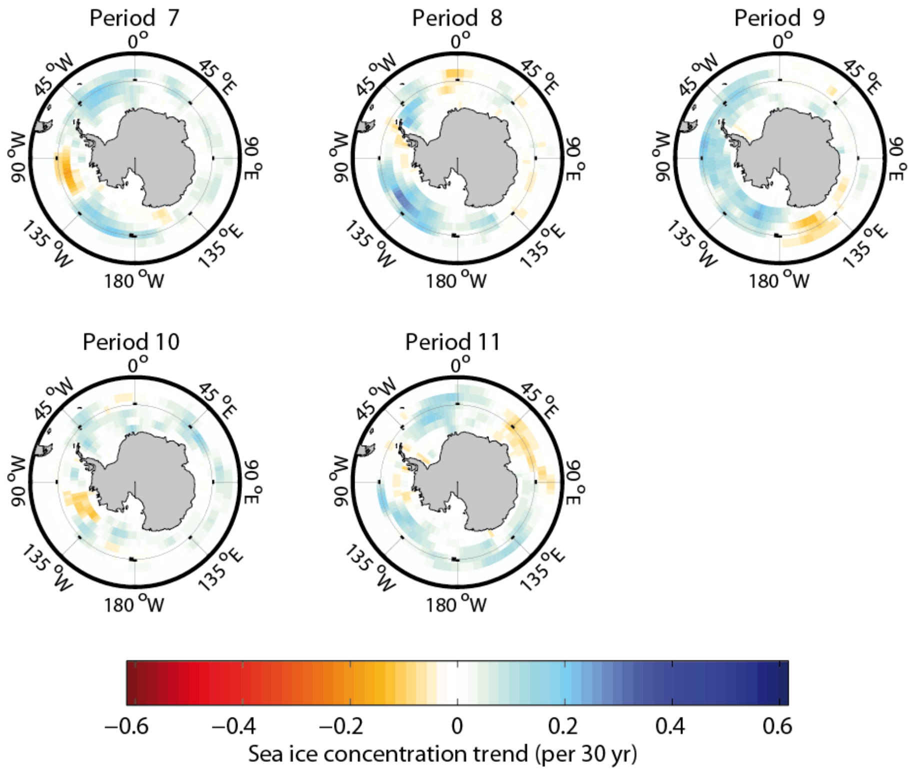

Fig. 6. Continued.

TCD
7, 4585–4632, 2013

Title Page
Abstract Introduction
Conclusions References
Tables Figures
◀| |▶
◀ ▶
Back Close
Full Screen / Esc
Printer-friendly Version
Interactive Discussion

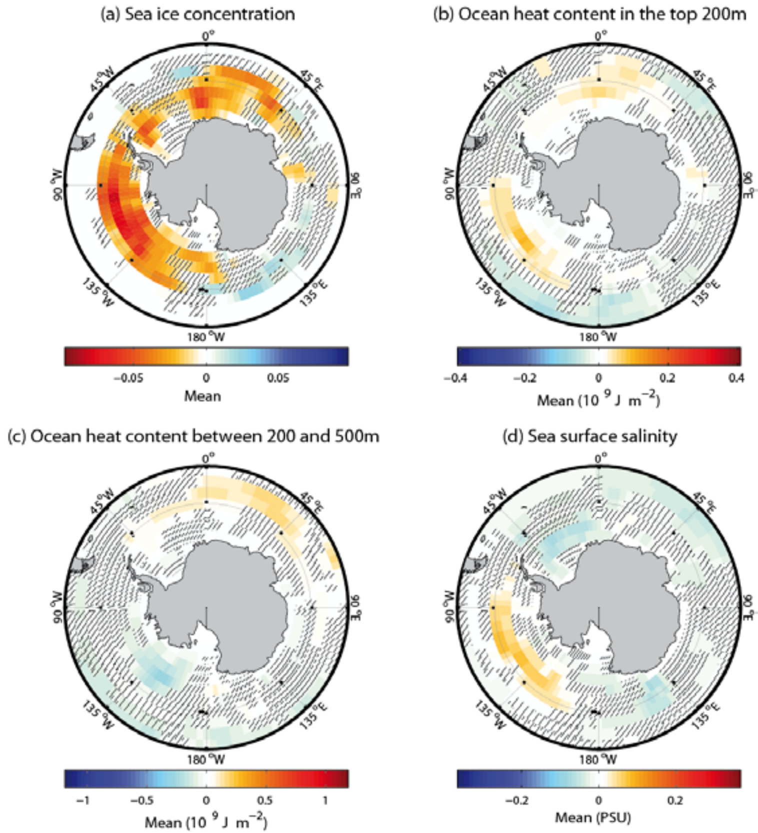

Fig. 7. Averages over the first year of the 11 periods showing a large increase in Antarctic sea ice extent of **(a)** ice concentration, **(b)** ocean heat content in the top 200 m ($J\,m^{-2}$), **(c)** ocean heat content in the layer between 200 and 500 m (in $J\,m^{-2}$), **(d)** sea surface salinity. The hatched areas represent the regions for which the mean value over the 11 periods is not significantly different at the 95 % level compared to periods not showing a large increase in ice extent.

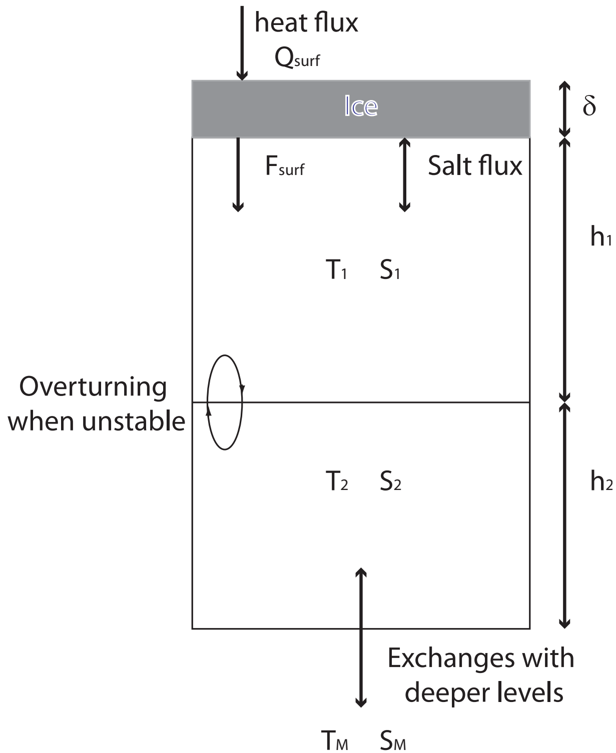

Fig. 8. Schematic representation of the two-layer model displaying the dominant processes included and the state variables.

TCD
7, 4585–4632, 2013

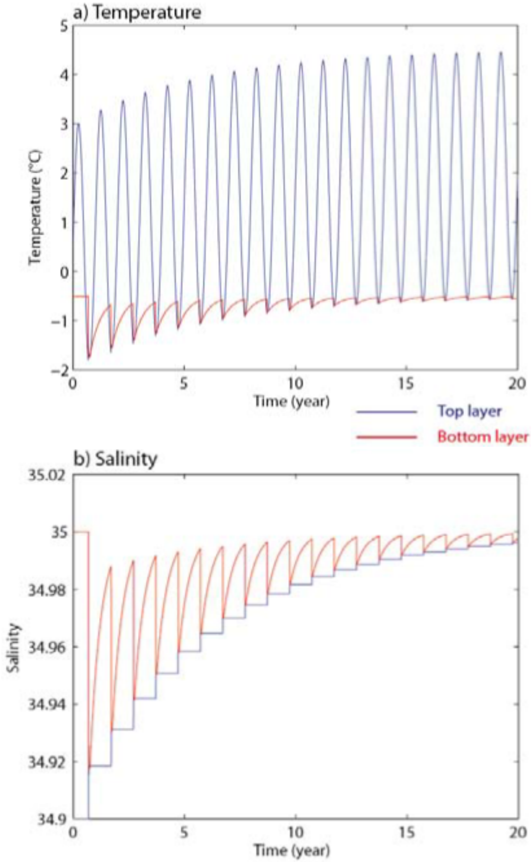

Fig. 9. (a) Temperature (K) and **(b)** salinity in an experiment performed with the two-layer model initialized from a weakly stratified state. The value of the top layer is in blue, the bottom one is in red.

TCD
7, 4585–4632, 2013

Decadal trends in the Antarctic sea ice extent

H. Goosse and V. Zunz

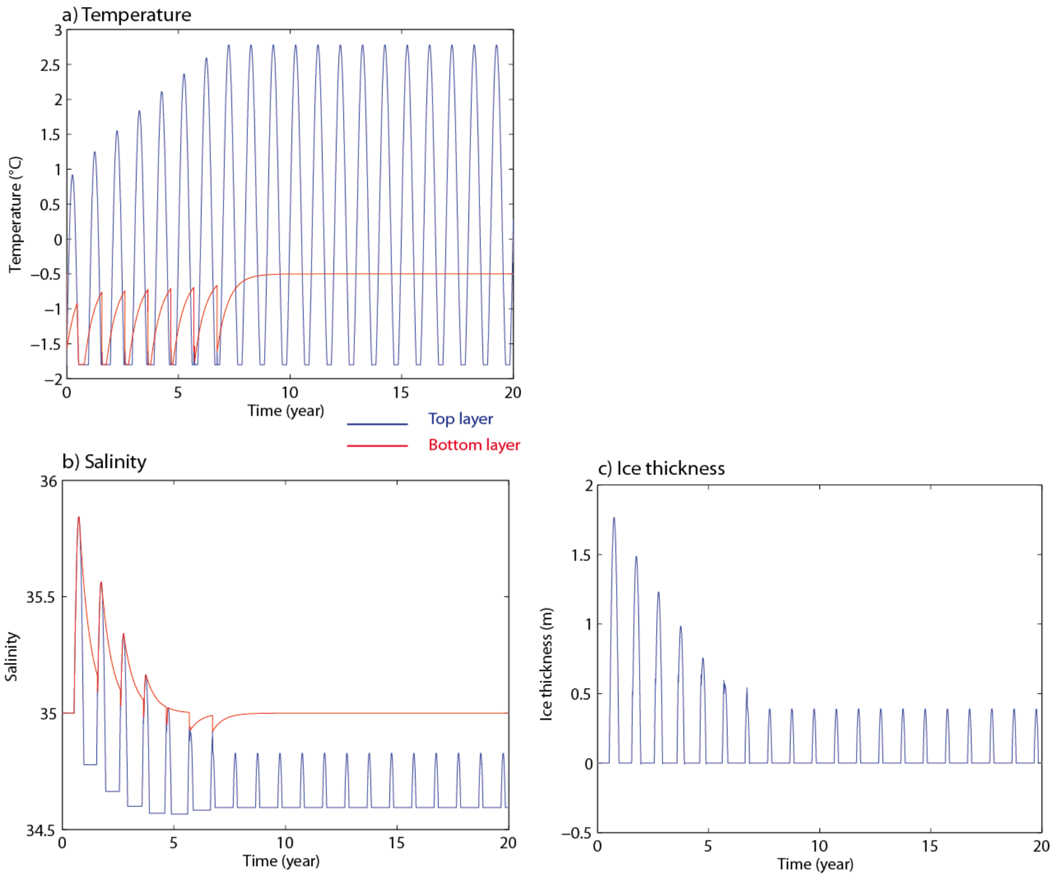

Fig. 10. (a) Temperature (K), **(b)** salinity, and **(c)** sea ice thickness (m) in the two-layer model after an instantaneous reduction of the temperature in the surface layer. The value of the top layer is in blue, the bottom one is in red.

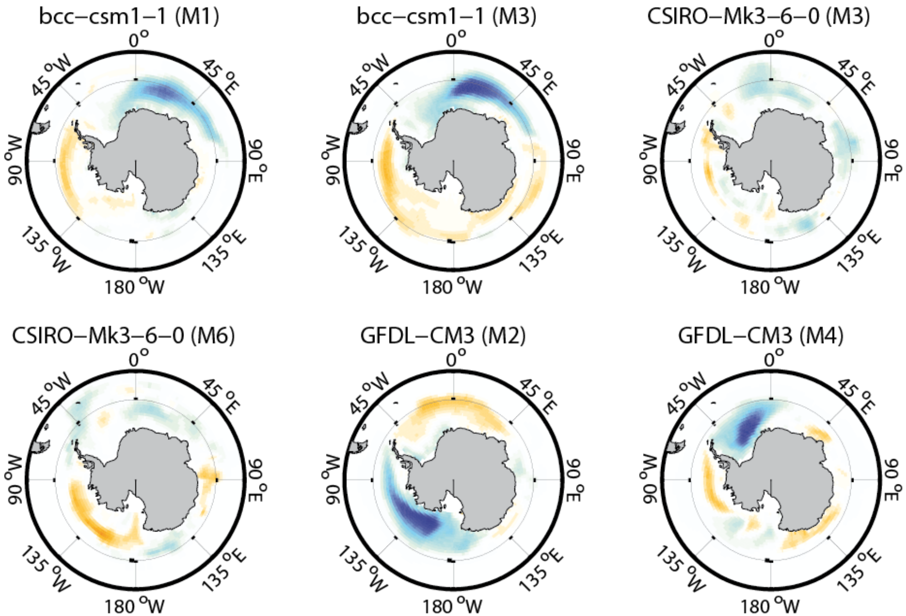

Fig. 11. Ice concentration trends over the period 1979–2005 in historical simulations performed with CGCMs in the framework of CMIP5. Only the simulations characterized by an increase in sea ice extent over this period are represented here. The trends are scaled to represent the 27 yr changes. The name of the model (Table 3) and the corresponding member of the ensemble (if several members are available in CMIP5 archive) are mentioned on the top of each panel.

TCD
7, 4585–4632, 2013

Decadal trends in the Antarctic sea ice extent

H. Goosse and V. Zunz

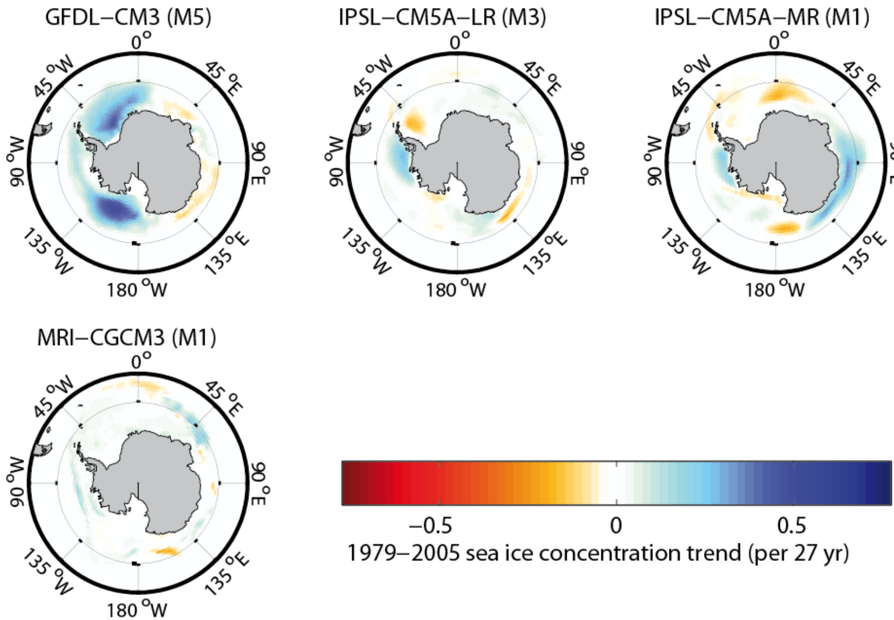

Fig. 11. Continued.

TCD
7, 4585–4632, 2013

Decadal trends in the Antarctic sea ice extent

H. Goosse and V. Zunz

Title Page
Abstract Introduction
Conclusions References
Tables Figures
◀| |▶
◀ ▶
Back Close
Full Screen / Esc
Printer-friendly Version
Interactive Discussion

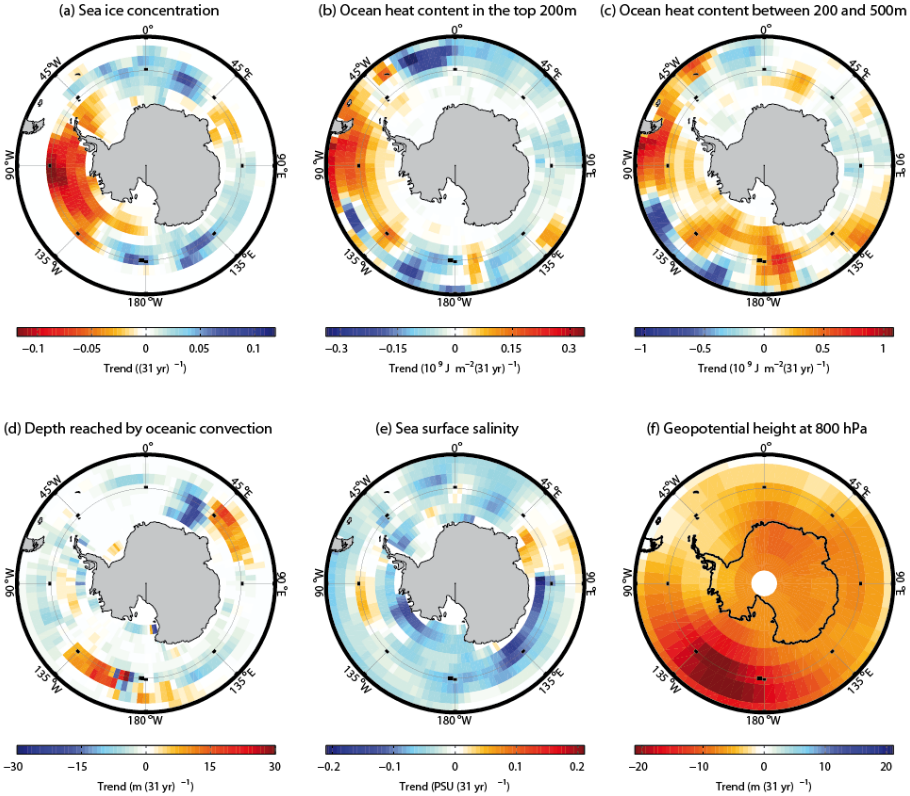

Fig. 12. Trends over the period 1979–2009 in a simulation with LOVECLIM using data assimilation scaled to represent the 31 yr changes of **(a)** ice concentration, **(b)** ocean heat content in the top 200 m ($J\,m^{-2}$), **(c)** ocean heat content in the layer between 200 and 500 m ($J\,m^{-2}$), **(d)** depth reached by oceanic convection (m), **(e)** sea surface salinity, **(f)** geopotential height at 800 hpa (m).

TCD

7, 4585–4632, 2013

Decadal trends in the Antarctic sea ice extent

H. Goosse and V. Zunz